

α_1 Adrenoceptor subtype selectivity 3D-QSAR models for a new class of α_1 adrenoceptor antagonists derived from the novel antipsychotic sertindole

Thomas Balle^{a,b}, Kim Andersen^a, Karina Krøjer Søby^c, Tommy Liljefors^{b,*}

^a Medicinal Chemistry Research, H. Lundbeck A/S, 9 Ottiliavej, 2500 Valby, Denmark

^b Department of Medicinal Chemistry, The Royal Danish School of Pharmacy, 2 Universitetsparken, 2100 Copenhagen, Denmark

^c Biological Research, H. Lundbeck A/S, 9 Ottiliavej, 2500 Valby, Denmark

Received 9 July 2002; received in revised form 17 December 2002; accepted 10 January 2003

Abstract

Receptor-binding affinities for the α_1 adrenoceptor subtypes α_{1a} , α_{1b} and α_{1d} for a series of 39 α_1 adrenoceptor antagonists derived from the antipsychotic sertindole are reported. The SAR of the compounds with respect to affinity for the α_{1a} , α_{1b} and α_{1d} adrenoceptor subtypes as well as affinity obtained by an α_1 assay (rat brain membranes) were investigated using a 3D-QSAR approach based on the GRID/GOLPE methodology. Good statistics ($r^2 = 0.91$ – 0.96 ; $q^2 = 0.65$ – 0.73) were obtained with the combination of the water (OH2) and methyl (C3) probes. The combination of steric repulsion and electrostatic attractions explain the affinities of the included molecules. The adrenergic α_{1a} receptor seems to be more tolerant to large substituents in the area between the indole 5- and 6-positions compared to the adrenergic α_{1b} and α_{1d} receptor subtypes. There seems to be minor differences in the position of areas in the α_{1b} receptor compared to α_{1a} and α_{1d} receptors where electrostatic interaction between the molecules and the receptor (OH2 probe) contribute to increased affinity. These observations may be used in the design of new subtype selective compounds. In addition, the model based on biological data from an α_1 assay (rat brain membranes) resembles the model for the α_{1b} adrenoceptor subtype.

© 2003 Elsevier Science Inc. All rights reserved.

Keywords: α_1 Adrenoceptor antagonist; Subtype selectivity; 3D-QSAR; GRID; GOLPE; Sertindole; Antipsychotic

1. Introduction

The α_1 adrenergic receptors belong to the large superfamily of G-protein-coupled receptors and are subdivided into the α_{1a} , α_{1b} and α_{1d} adrenoceptor subtypes [1]. In human brain, these receptors are all present at the mRNA level [2]. At the protein level, radioligand binding experiments have confirmed the existence of the α_{1a} [3] and α_{1d} adrenoceptor subtypes [4]. Good correlations between receptor-binding affinities observed for the cloned α_{1a} (bovine), α_{1b} (hamster), α_{1d} (rat) receptors and the corresponding human clones have been documented [5].

Development of selective α_1 adrenoceptor antagonists have primarily focused on therapeutics for the treatment of cardiovascular diseases and benign prostatic hyperplasia [6–9]. However, modulation of α_1 adrenoceptor activity in the central nervous system (CNS) may also be of interest in connection with treatment of CNS-related diseases such

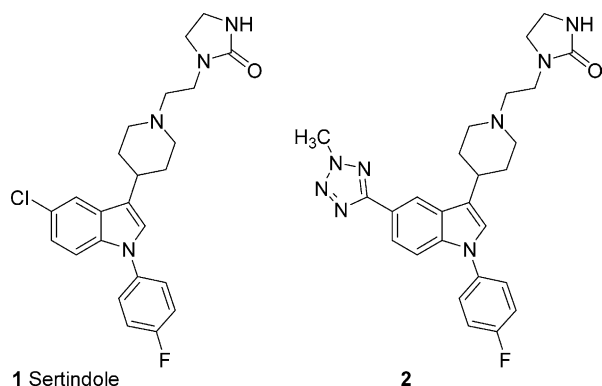
as schizophrenia, mania and post-traumatic stress disorder [10–12].

Most of the novel antipsychotics such as clozapine, sertindole (1), olanzapine and seroquel have nanomolar affinity for α_1 adrenoceptors in addition to their affinities for dopamine D₂ and serotonin 5-HT_{2a} receptors [13]. The importance of the α_1 component of these drugs have been studied intensively [10,14–17]. However, the role of the individual α_1 adrenoceptor subtypes, α_{1a} , α_{1b} and α_{1d} with respect to antipsychotic efficacy and adverse effects has received little attention. One reason for this may be the lack of truly subtype selective compounds with good blood–brain barrier penetration.

The novel antipsychotic sertindole (1, Scheme 1), has nanomolar affinity for adrenergic (α_1), dopaminergic (D₁–D₄) and serotonergic (5-HT_{2a} and 5-HT_{2c}) receptors [13]. In addition, Ipsen et al. [18] found that sertindole is a specific inhibitor of α_{1a} adrenoceptors in rat small arteries and binds with nanomolar affinity to the adrenergic α_{1a} receptor and with considerably lower affinity to the α_{1b} and α_{1d} receptors. However, in our hands, sertindole binds with

* Corresponding author.

E-mail address: tl@dfh.dk (T. Liljefors).

Scheme 1. Structures of compounds **1** and **2**.

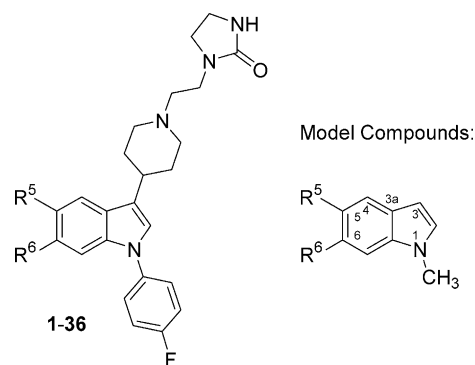
subnanomolar affinity to all three α_1 adrenoceptor subtypes [19].

We recently described the replacement of the chlorine atom in sertindole (**1**, Scheme 1), with heteroaryl-, carbamoyl- and aminomethyl substituents [20], resulting in a new class of selective α_1 adrenoceptor antagonists. One of these compounds, a 5-(2-methyltetrazol-5-yl) analogue **2** (Scheme 1) of sertindole (**1**), binds with 0.23 nM affinity for adrenergic α_{1a} receptors and has an overall selectivity of more than 208 times with regard to dopamine D_2 – D_4 and serotonin 5-HT $_{1a}$, 5-HT $_{1b}$, 5-HT $_{2a}$ and 5-HT $_{2c}$ receptors. The selectivity for the α_{1a} receptor with regard to the adrenergic α_{1b} and α_{1d} receptors is a factor of 5 and 8, respectively.

In this paper, we report receptor-binding affinities and 3D-QSAR models using the GRID [21,22]/GOLPE [23–25] procedure for 5- and 6-substituted analogues of sertindole (**1**) with respect to each of the adrenergic α_1 subtypes, α_{1a} , α_{1b} and α_{1d} . In addition, a 3D-QSAR model representing the α_1 receptors based on an assay consisting of rat brain membranes is reported and compared to the models obtained from the separate subtypes.

3D-QSAR methods applied to the description of selectivity between the individual α_1 adrenoceptor subtypes, α_{1a} , α_{1b} and α_{1d} have mainly been limited to the use of methods based on theoretical molecular descriptors applied across a variety of compounds belonging to different chemical classes [26–29]. The knowledge about how these different classes of compounds bind to the receptor is very limited even though site-directed mutagenesis studies of the receptors has started to shed light on this topic [30–33]. Recently, a new proteo-chemometric approach was introduced and tested in relation to a data set consisting of α_1 adrenoceptor antagonists [34].

The aim of the present work is to make a contribution to the understanding of the molecular features of the 5- and 6-substituted analogues of sertindole (**1**) that determines the selectivity for the different subtypes of the adrenergic α_1 receptors. Such an understanding may give a basis for the design of novel subtype selective α_1 adrenoceptor antagonists.

Scheme 2. Generic structure for compounds **1–36** listed in Table 1 and generic structure for model compounds **1–36** used for calculating 3D-QSAR model.

2. Methods

2.1. Training set and validation set

The 3D-QSAR models are based on a training set of 36 previously reported compounds **1–36** [19,20,35–38] (Scheme 2 and Table 1). A validation set consisting of three previously reported compounds **37–39** [20,38] (Table 2), was used for external validation. These compounds are structurally dissimilar to the compounds in the training set and, furthermore, do not have the same problems regarding conformational properties. Consequently, they are well suited to reflect the true performance of the models. The compounds are restricted to contain structural variation in the indole 5- and 6-positions only, thus forming a homogenous set. In addition, all pharmacological data were obtained from the same laboratory, eliminating the potential noise that may be introduced by pooling of data sets from different sources.

2.2. Model compounds

Conformational analysis showed that the substituents in the indole 5- and 6-positions of the compounds **1–39** had virtually no effect on the conformation of the 3-piperidinyl side chain and on the 1-(4-fluorophenyl) substituents on the indole skeleton. These substituents are conserved among all molecules included in the model and are, therefore, not considered to contribute to the description of the differences in the observed affinity. These substituents were consequently not included in the model. Instead, a set of reduced model compounds were used (Scheme 2), where the substituent in the indole 3-position was replaced with a hydrogen and the indole N1-substituent was replaced with a methyl group. Conformational analysis on the reduced model compounds were performed using the MMFFs [39] force-field and the GB/SA solvation model as implemented in MacroModel [40] by systematic dihedral driving (increment: 10°) on the non-protonated species.

Table 1

Receptor-binding affinities for α_1 adrenergic receptors for 5- or 6-substituted 1-(4-fluorophenyl)-1*H*-indoles 1–36 (Scheme 2) included in 3D-QSAR model^a

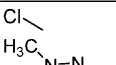
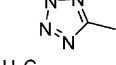
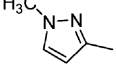
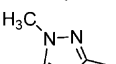
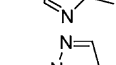
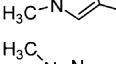
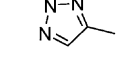
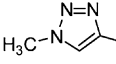
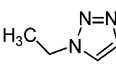
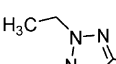
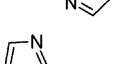
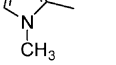
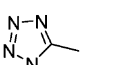
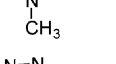
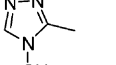
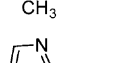
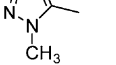
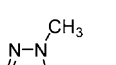
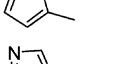
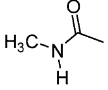
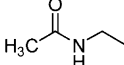
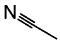
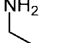
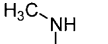
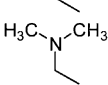
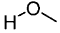
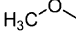
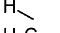
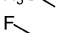
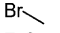
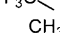
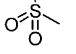
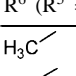

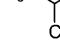
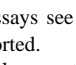
Compound	R ⁵ (R ⁶ = H)	K _i (nM)				Reference
		α_1	α_{1a}	α_{1b}	α_{1d}	
1		1.4	0.37	0.33	0.66	[19] ^b
2		1.8	0.23	1.1	2.0	[19] ^b
3		3.7	0.49	4.0	4.8	[19] ^b
4		2.5	0.80	6.9	5.9	[19] ^b
5		22	6.8	3.8	8.6	[19] ^c
6		1.7	1.4	0.74	1.7	[19] ^c
7		9.5	3.0	6.0	8.6	[19] ^c
8		11	4.2	6.0	19	[19] ^c
9		4.4	1.5	0.65	2.9	[19] ^c
10		1.2	1.4	3.3	3.5	[19] ^c
11		1.3	1.5	2.0	6.6	[19] ^c
12		6.8	6.2	10	13	[19] ^c
13		0.45	0.42	1.3	1.3	[19] ^c
14		3.0	3.6	2.0	5.5	[19] ^c
15		1.2	3.2	1.4	3.1	[19] ^c
16		2.0	0.68	2.1	2.3	[19] ^c
17		3.2	1.6	2.3	2.7	[19] ^c
18		5.3	1.8	1.1	4.1	[19] ^c
19		3.9	2.1	12	29	[20] ^b

Table 1 (Continued)

Compound	R ⁵ (R ⁶ = H)	K _i (nM)				Reference
		α ₁	α _{1a}	α _{1b}	α _{1d}	
20		2.5	3.7	4.4	14	[20] ^b
21		0.46	0.68	1.0	2.9	[20] ^c
22		0.46	0.09	0.25	0.62	[35]
23		0.50	0.18	1.1	0.69	[20] ^b
24		0.45	0.80	0.60	0.48	[20] ^c
25		0.58	0.60	0.18	0.59	[20] ^b
26		0.18	0.17	0.13	0.30	[37]
27		1.3	0.17	1.1	1.6	[35]
28		0.63	0.26	0.74	0.72	[35]
29		1.5	0.22	0.51	1.0	[35]
30		1.0	0.24	0.51	1.5	[35]
31		2.0	0.54	0.60	3.8	[35]
32		3.0	0.68	0.36	1.8	[35]
33		0.58	0.25	0.93	1.5	[35]
R ⁶ (R ⁵ = H)						
34		22	1.4	18	21	[36] ^d
35		18	4.2	33	62	[38]
36		280	40	140	520	[36] ^d

^a For description of assays see Section 3.6.^b Data previously reported.^c Data for α₁ previously reported.^d Data for α₁ previously reported as IC₅₀ value.

2.3. Alignment

In the alignment, it was assumed that all molecules bind to the different receptor subtypes in a similar mode. The substituents in the indole 5-position may be aligned according to steric or electrostatic properties. In the present work we have chosen to superimpose electrostatic features (lonepairs) of the substituents and to direct these towards the indole 4-position. This was encouraged by the similar receptor-binding affinities noticed by comparing the 5-methoxy substituted compound **27** (Table 1), and the 5,6-methylenedioxy-substituted compound **38** (Table 2). The oxygen and the carbon of the two substituents can be superimposed in only one way, resulting in a common lonepair direction pointing in the direction of the indole 4-position. As a consequence, all compounds were aligned with the lonepairs pointing in this direction if possible.

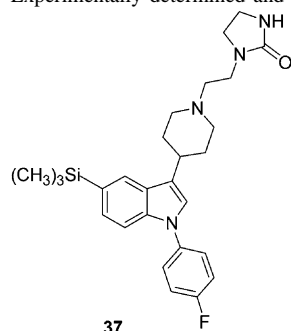
The 5-(1-methylpyrazol-3-yl)-substituted compound **3** was used as template in a conformation where the sub-

stituent was coplanar with the indole. The lonepair of the pyrazole 2-position was oriented in the direction of the indole 4-position. The remaining compounds were superimposed on the low energy conformation (<1 kcal/mol above global minimum) giving the best fit of the direction of a lonepair to the direction of the lonepair of the template. Compounds **2** and **4** were oriented with the nitrogen having the highest electron density (based on semi-empirical AM1 calculations) towards the indole 4-position. The compounds were aligned as they are depicted in Table 1 if not explicitly discussed in the text below. Dihedral angles of the fitted compounds are reported in Table 3. Further alignment was performed as follows: The ethyl groups of the substituents in compounds **8** and **9** were directed below the plane of the indole skeleton. The substituent in compound **21** was in an extended conformation, and the substituents of **23–25** oriented with the lonepair of the nitrogen in the direction of the lonepair of the template molecule. The substituent of compound **33** was oriented with the methyl group above the

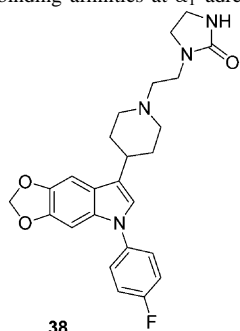
Table 2

Experimentally determined and calculated receptor-binding affinities at α_1 adrenergic receptors for the external test set **37–39**

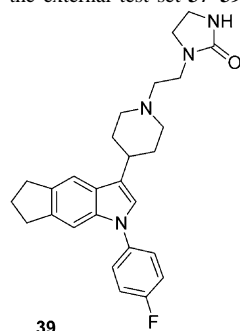
experimentally determined K_i values for the α_1 and α_{1d} receptors binding animals at 100 nM. The α_{1b} and α_{1a} receptors for the internal test set



37



38



39

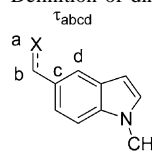
Compound	Predicted K_i (nM)				Measured K_i (nM)				Reference
	α_1	α_{1a}	α_{1b}	α_{1d}	α_1	α_{1a}	α_{1b}	α_{1d}	
37	6.2	3.8	1.9	7.5	24 ^a	1.9	6.0	6.6	[20]
38	2.8	0.38	2.5	3.5	0.52 ^a	0.19	0.69	3.3	[20]
39	37	2.6	11	34	21	1.2	4.4	30	[38]

^a Data previously reported.

plane of the indole. The substituent of compound **36** was oriented with the methyl groups towards the indole 5-position. The model compounds were fitted on basis of the rigid indole skeleton present in all molecules. The indole C5, C3a and N1 atoms (for definition see Scheme 2) were used as fitting points, and a rigid body fitting procedure was applied.

Table 3

Definition of dihedral angles used for superimposition of molecules

	X = N:	2-4, 6-13, 16
	X = CH:	5, 15, 17-18
	X = N-CH ₃ :	14
	X = O:	19-20
	X = NR ₁ R ₂ :	21, 23-25

Compound	τ_{abcd}
2	0.07
3	0.12
4	0.04
5	21.5
6	0.11
7	0.04
8	0.04
9	0.94
10	48.5
11	42.0
12	49.0
13	44.0
14	56.1
15	49.3
16	0.02
17	44.6
18	47.1
19	60.0
20	26.9
21	89.0
23	84.2
24	84.6
25	64.4

3. 3D-QSAR

3.1. GRID calculations

To mimic the possible interactions of the compounds with the receptor, the interaction energies with three different probes, OH2, C3 and N1+ were calculated using the program GRID version 19 [21,22]. The probes represent a water molecule, a methyl group and a positively charged NH⁺ group. Calculations with a grid spacing of 1 Å and the grid dimensions (Å): X_{\min}/X_{\max} , $-5/18$; Y_{\min}/Y_{\max} , $-3/16$; and Z_{\min}/Z_{\max} , $-2/15$ resulted in 8640 X-values per probe for each molecule.

3.2. Data pre-treatment

GOLPE automatically deletes X-variables with values $<1.0E-7$. Further pre-treatment was performed as follows: X-values lower than 0.05 were set to zero. X-values with variance below 0.1 were deleted (minimum S.D. cut-off = 0.1) for all probes. Second and third level X-variables were deleted. Pre-treatment reduced the number of variables to approximately 10% (for details see Table 4) of the original number without significantly affecting the predictive ability of the model. Initial models were built on these data.

3.3. Choice of probes

The effect of the three different probes, OH2, C3 and N1+, were evaluated both alone and in combination. Only results obtained from a combination of the C3 and OH2 probes and from the C3 probe alone are reported. Models including all three probes had slightly lower predictive

Table 4
Properties of 3D-QSAR models for adrenergic α_{1a} , α_{1b} , α_{1d} and α_1 affinities

	Initial models				Models after SRD and FFD				
	No. of variables ^a	No. of LVs	r^2	q^2	No. of variables	No. of LVs	r^2	q^2	SDEP ^b
OH2 and C3 probes (17,280) ^c									
α_1	1736	5	0.95	0.60	1019	5	0.95	0.73	0.56
α_{1a}	1736	4	0.90	0.48	1004	4	0.91	0.65	0.31
α_{1b}	1736	5	0.94	0.50	916	5	0.96	0.72	0.48
α_{1d}	1736	5	0.94	0.45	929	5	0.95	0.67	0.07
C3 probe (8640) ^c									
α_1	800	5	0.90	0.46	473	5	0.91	0.62	0.70
α_{1a}	800	4	0.86	0.41	404	4	0.88	0.59	0.33
α_{1b}	800	5	0.91	0.55	467	5	0.92	0.69	0.57
α_{1d}	800	5	0.92	0.49	478	5	0.92	0.64	0.20

^a Variables after pre-treatment.

^b Standard deviation on error of prediction (SDEP) for external validation set **37–39** (\log_{10} units), $SDEP = (\sum (Y_{\text{exp}} - Y_{\text{calc}})^2 / N)^{1/2}$.

^c Variables before pre-treatment.

ability compared to models based on a combination of the C3 and OH2 probes.

3.4. Variable reduction

Further refinement of data involving smart region definition (SRD) [41] and fractional factorial design (FFD) [25] was performed.

Groups of variables were generated using the default number of seeds. Variables with a distance < 1 Å were included in the groups. Groups within a distance of less than 2 Å containing the same information were collapsed. The groups of variables were used in the calculations instead of individual variables.

The effect of the individual groups on the predictive ability of the model was evaluated using the FFD procedure implemented in GOLPE. The effect of dummy variables (20%) on the predictive ability of the model was evaluated. Only groups having a positive influence on the predictive ability larger than the average dummy variable were included in the final model.

3.5. PLS models

One PLS model correlating the observed affinities for each of the three adrenergic receptor subtypes, α_{1a} , α_{1b} and α_{1d} with the predictors (X -variables), was built. In addition, one model correlating the observed affinities in the α_1 assay (rat brain membranes) with the predictors (X -variables) was built. Dependent variables (Y -variables) were entered unscaled as pK_i values.

Cross-validation was performed by 20-fold repetition of the “leave 5 random groups out” procedure, resulting in 100 reduced models. The reduced models were used to calculate the affinity of the molecules left out. The complete models were finally used to calculate the affinities of the external validation set consisting of three compounds **37–39** (Table 2).

3.6. Pharmacology

The experimental data in Tables 1 and 2 have only been published in part [19,20,36]. A detailed description of the assays used to determine affinity for α_1 (rat brain homogenate), α_{1a} (bovine, recombinant), α_{1b} (hamster, recombinant) and α_{1d} (rat, recombinant) receptors may be found in the literature [19]. Standard errors for experimentally determined pK_i values are within 0.3 for $n \geq 2$. The data are not explicitly discussed below unless supporting a trend observed in the 3D-QSAR models.

4. Results and discussion

4.1. PLS models

PLS models based on four or five latent variables (LVs) gave the best statistical properties and the best prediction of the affinities of the external validation set. For the α_{1a} model, predictive ability (q^2) decreased after the fourth LV. For the remaining models, no significant increase in predictive ability was observed after the fifth LV.

The statistics of PLS models correlating the receptor-binding affinities for the adrenergic α_{1a} , α_{1b} and α_{1d} as well as α_1 receptors with the three-dimensional molecular descriptors obtained from GRID is reported in Table 4 for models based on a combination of the C3 and OH2 probes as well as for the C3 probe alone. In Table 5, experimentally determined and calculated receptor-binding affinities expressed as pK_i values for the models based on the combination of the C3 and OH2 probes are listed. In Fig. 1, these data are presented graphically. In Table 2, experimentally determined and calculated receptor-binding affinities for the compounds included in the external test set (**37–39**) are reported as K_i values.

The models based on the C3 and OH2 probes have the highest quality. The initial models (Table 4) explained most

Table 5

Experimentally determined and calculated receptor-binding affinities for compounds **1–39** (pK_i values)^{a,b}

Compound	α_1		α_{1a}		α_{1b}		α_{1d}	
	Experimental	Calculated	Experimental	Calculated	Experimental	Calculated	Experimental	Calculated
1	8.85	8.95	9.43	9.68	9.48	9.42	9.18	9.07
2	8.75	8.93	9.64	9.53	8.96	8.93	8.70	8.85
3	8.43	8.47	9.31	9.03	8.40	8.38	8.32	8.31
4	8.60	8.70	9.10	9.38	8.16	8.45	8.23	8.52
5	7.66	7.63	8.17	8.19	8.42	8.37	8.07	7.94
6	8.77	8.75	8.85	9.11	9.13	8.87	8.77	8.62
7	8.02	7.90	8.52	8.45	8.22	8.17	8.07	7.95
8	7.96	7.98	8.38	8.51	8.22	8.35	7.72	7.78
9	8.36	8.30	8.82	8.89	9.19	9.19	8.54	8.38
10	8.92	8.76	8.85	8.79	8.48	8.35	8.46	8.36
11	8.89	8.95	8.82	8.76	8.70	8.77	8.18	8.44
12	8.17	8.56	8.21	8.53	8.00	8.20	7.89	8.10
13	9.35	9.18	9.38	9.98	8.89	8.92	8.89	8.72
14	8.52	8.42	8.44	8.30	8.70	8.72	8.26	8.22
15	8.92	8.93	8.50	8.68	8.85	8.91	8.51	8.53
16	8.70	8.66	9.17	9.14	8.68	8.58	8.64	8.61
17	8.50	8.55	8.80	8.77	8.64	8.84	8.57	8.63
18	8.28	8.28	8.75	8.60	8.96	8.74	8.39	8.39
19	8.41	8.39	8.68	8.66	7.92	7.70	7.54	7.45
20	8.60	8.47	8.43	8.60	8.36	8.26	7.85	7.73
21	9.34	9.35	9.17	9.06	9.00	9.05	8.54	8.54
22	9.34	9.19	10.05	9.85	9.60	9.57	9.21	9.03
23	9.30	9.18	9.75	9.63	8.96	8.96	9.16	9.12
24	9.35	9.30	9.10	9.18	9.22	9.21	9.32	9.27
25	9.24	9.25	9.22	9.10	9.75	9.87	9.23	9.31
26	9.75	9.61	9.77	9.94	9.89	9.65	9.52	9.43
27	8.89	8.78	9.77	9.57	8.96	8.94	8.80	8.64
28	9.20	9.10	9.59	9.53	9.13	9.11	9.14	8.97
29	8.82	8.87	9.66	9.61	9.29	9.38	9.00	9.03
30	9.00	9.34	9.62	9.75	9.29	9.42	8.82	9.19
31	8.70	8.79	9.27	9.54	9.22	9.32	8.42	8.83
32	8.52	8.46	9.17	9.22	9.44	9.34	8.75	8.66
33	9.24	9.13	9.60	9.55	9.03	9.09	8.82	8.77
34	7.66	7.70	8.85	8.69	7.75	7.81	7.68	7.66
35	7.75	7.59	8.38	8.29	7.48	7.48	7.21	7.20
36	6.55	6.65	7.40	7.53	6.85	6.92	6.28	6.42
37	7.62	8.21	8.72	8.42	8.22	8.71	8.18	8.13
38	9.28	8.55	9.72	9.42	9.16	8.61	8.48	8.39
39	7.68	7.43	8.92	8.59	8.36	7.98	7.52	7.46

^a References to previously reported data are listed in Table 1.^b Models based on C3 and OH2 probes.

of the variance in data ($r^2 = 0.90$ – 0.95), and the models had moderate predictive abilities ($q^2 = 0.45$ – 0.60). The variable selection procedure (SRD and FFD) resulted in a significant increase in predictive abilities ($q^2 = 0.65$ – 0.73). In contrast, r^2 was not significantly affected ($r^2 = 0.91$ – 0.96).

PLS models based on the C3 probe alone have, after variable selection procedures, a slightly lower quality ($r^2 = 0.88$ – 0.92 ; $q^2 = 0.59$ – 0.64) compared to the models based on two probes. The minor differences between the two sets of models indicate that steric interactions play a major role in describing the variance in receptor-binding affinities. The differences in predictive abilities (q^2) between the models based on a combination of the C3 and OH2 probes and the models based on the C3 probe alone were most pronounced for the model representing α_1 and α_{1a} (difference = 0.11

and 0.06) and less pronounced for the models representing α_{1b} and α_{1d} (both 0.03).

The plots of experimentally determined affinity versus calculated affinity (Fig. 1) show a good correlation and indicate a good prediction of the affinity of the external validation set **37–39** (Table 2). The standard deviation on error of prediction (SDEP, Table 4) for the four models were in the range of 0.07–0.56 log₁₀ units. The largest deviation was noted for the α_1 model, which was also expected because of the complex nature of the rat brain homogenate compared to the isolated recombinant receptors expressed in cell lines. As apparent from the data in Table 4, the SDEP for the models based on the C3 probe alone was slightly higher compared to the models based on a combination of the C3 and OH2 probes indicating some importance of the electrostatic interactions.

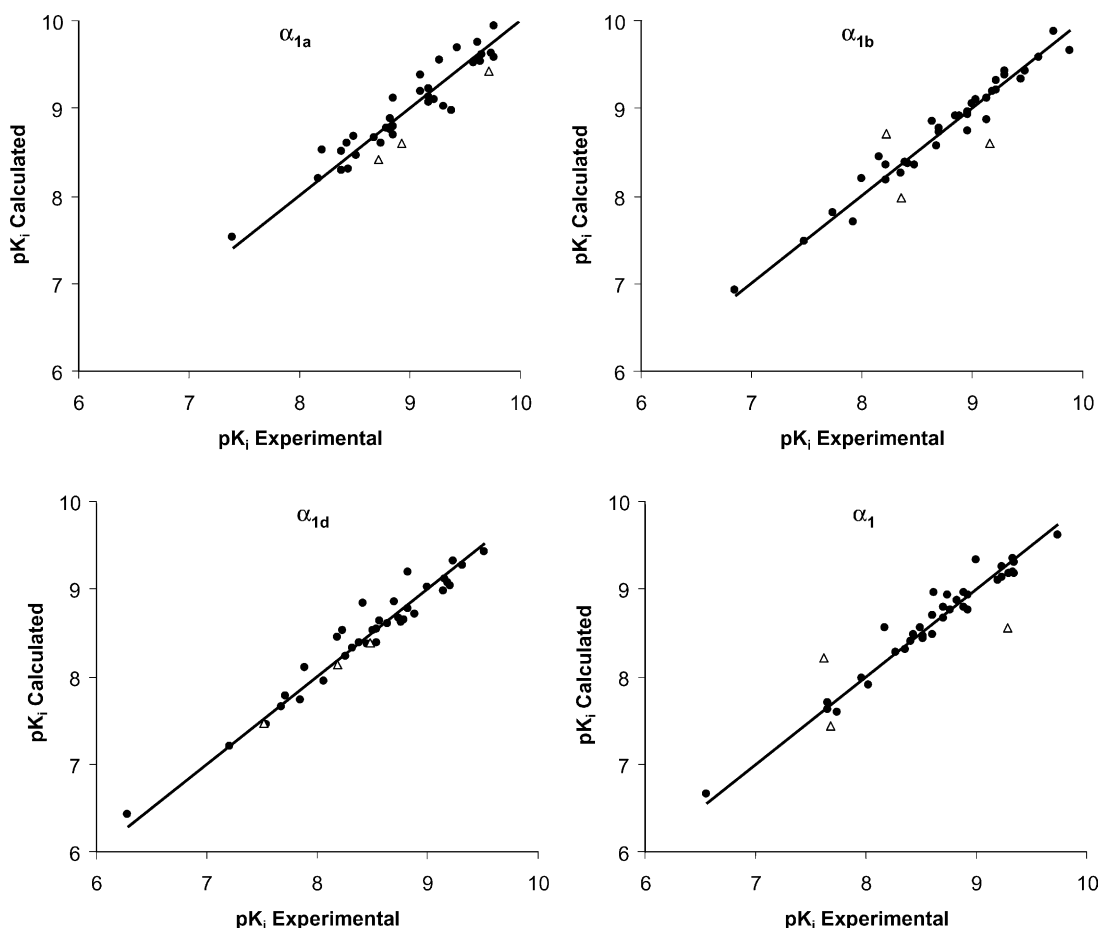


Fig. 1. Experimental vs. calculated affinities (pK_i) at adrenergic α_{1a} , α_{1b} , α_{1d} and α_1 receptors: (●) training set; (△) validation set. Models based on the C3 and OH2 probes.

5. Interpretation of contour maps

Contour maps connecting grid points at the same level for models based on five LVs (four LVs, α_{1a}) for the models obtained using a combination of the C3 and OH2 probes are presented in Figs. 2 and 3 for the two probes, respectively. Within each figure, coefficients are set to the same value to allow for comparison between models.

5.1. C3 contour maps

Contour maps of the PLS coefficients for the four different adrenergic models for the C3 probe are shown in Fig. 2. The plots show a clear difference between the models for the three adrenergic α_1 subtypes, α_{1a} , α_{1b} and α_{1d} . The area representing negative coefficients (shown in blue) increases from α_{1a} over α_{1b} to α_{1d} . An unfavourable interaction (positive interaction energy, i.e. steric repulsion) between a substituent in the molecule and the C3 probe in the areas with negative coefficients is predicted to result in decreased affinity (decreased pK_i value). Thus, the adrenergic α_{1a}

receptor seems to accommodate larger substituents in the area corresponding to the indole 6-position compared to the other two receptor subtypes. This effect is clearly observed by comparing the affinity for the 6-methyl-substituted compound **34** with the unsubstituted **28** (Table 1). The affinity for adrenergic α_{1a} receptors is lower by a factor of 5 in the 6-methyl analogue **34**. In comparison, the affinity of compound **34** for the α_{1b} and α_{1d} receptor subtypes is lower by a factor of 24 and 29, respectively, compared to compound **28**.

In areas corresponding to positive coefficients (shown in red), an unfavourable interaction (positive interaction energy, i.e. steric repulsion) between a substituent in the molecule and the probe is predicted to lead to increased affinity (increased pK_i value). The areas of positive coefficients occupy similar positions in space, and the size increases from α_{1a} over α_{1d} to α_{1b} . In addition, the plot of positive coefficients for the α_{1b} model shows an isolated area marked with a black arrow. However, adjustment of the contour levels reveals that this area is of low significance compared to the area surrounding the methyl substituent of the *N*-methyl-pyrazole **3** shown as a template.

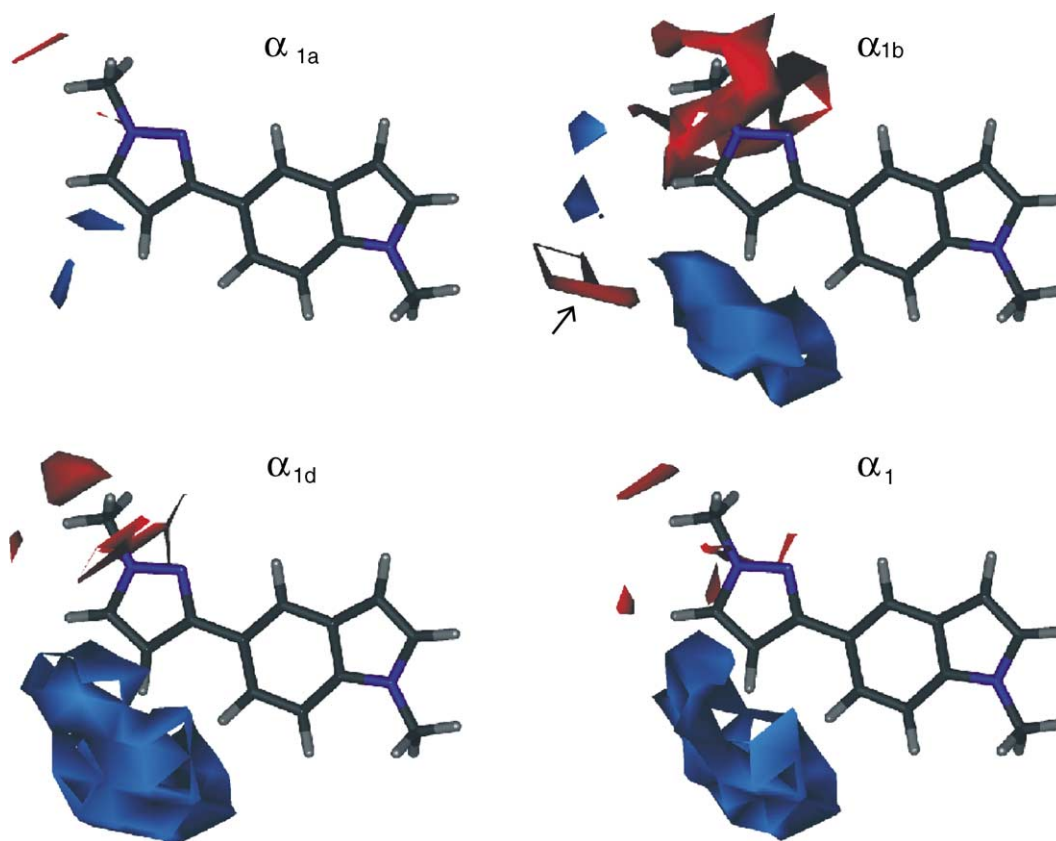


Fig. 2. Contour maps for affinity at adrenergic α_{1a} , α_{1b} , α_{1d} and α_1 receptors. Positive coefficients (red, 0.002 level) and negative coefficients (blue, -0.0035 level) for interaction with the methyl probe (C3) are shown. An unfavourable interaction (positive interaction energy, i.e. steric repulsion) between a substituent and the probe in regions with negative coefficients is predicted to decrease the affinity (decrease pK_i) and vice versa for positive coefficients. The 5-(1-methylpyrazol-3-yl)-substituted compound **3** is drawn to illustrate the size of the regions.

The results indicate that the affinity for α_{1b} receptors will benefit most from small alkyl substituents in the indole 5-position. The effect is clearly observed by comparing the 6-methyl-substituted compound **34** with the 5,6-propano derivative **39**. The latter have enhanced affinity for α_{1b} receptors compared to **34**, whereas the affinities for the remaining receptor subtypes are decreased.

5.2. OH2 contour maps

Contour maps of the PLS coefficients for the four different adrenergic models for the OH2 probe are shown in Fig. 3. The contribution of the OH2 probe to the PLS models is ambiguous since this probe, apart from a steric component, contains both a hydrogen bond donating and a hydrogen bond accepting component.

Adjustment of the contour levels for the PLS coefficients for the C3 and OH2 probes showed that the majority of the areas of positive and negative coefficients for the two probes occupy similar positions in space. This indicates that the major effect of the OH2 probe is of steric nature.

However, there are small areas of high significance marked with black arrows in the contour plots for the

OH2 probe where they differ significantly from the plots representing interactions with the C3 probe.

Comparison with models also including the N1+ probe which, apart from the steric component, may only serve as a hydrogen bond donor, revealed that these areas were also present at similar positions in space in the contour maps of the PLS coefficients for the N1+ probe (not shown).

Therefore, these distinct areas of negative coefficients (shown in blue) must represent specific electrostatic interactions with the hydrogen bond donating a component of the OH2 probe. A favourable interaction (negative interaction energy, i.e. electrostatic attraction) between a substituent in the molecule and the probe in these areas is predicted to lead to increased affinity (increased pK_i value). The effect of the specific electrostatic interactions may be exemplified by comparing the 5,6-propano derivative **39** with the 5,6-methylenedioxy compound **38**. The latter compound has enhanced affinity for all three adrenoceptor subtypes with a factor of 6–9.

These areas are located approximately 1.8 \AA from the position of the oxygen in the 5-hydroxy compound **26**, indicating that the areas represent the position of a specific hydrogen bond donor in the receptor. The exact position

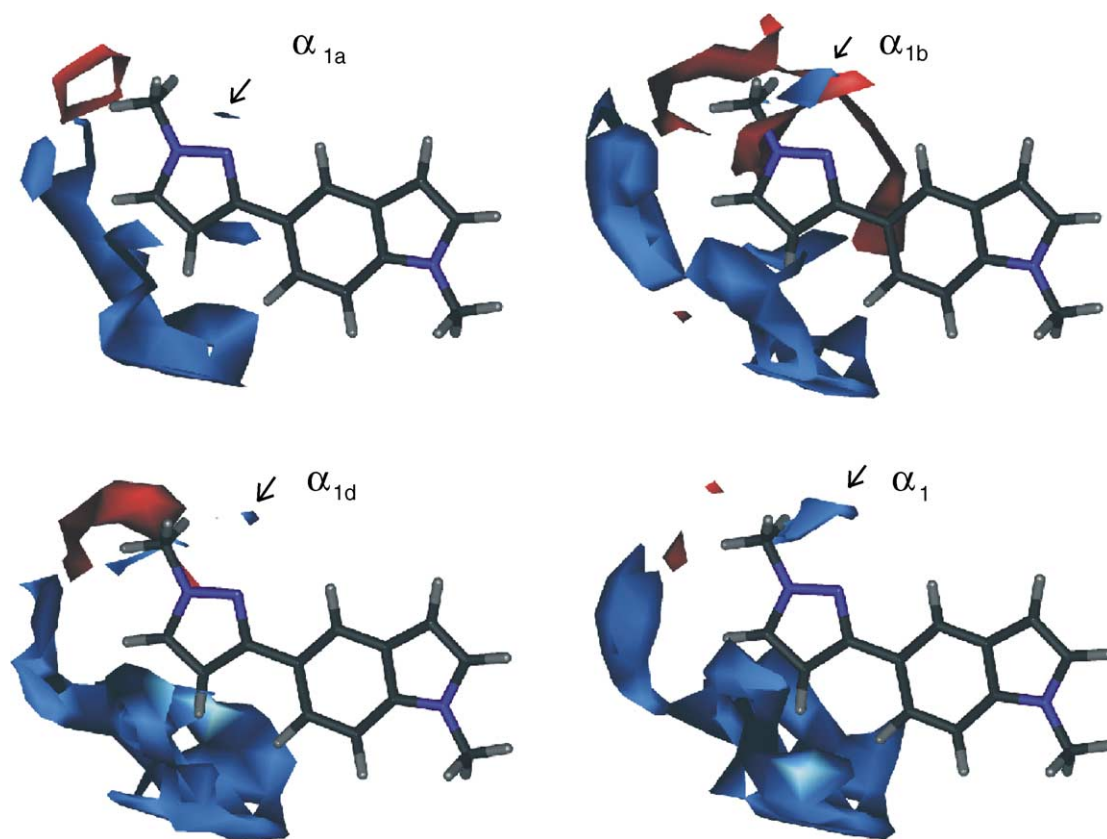


Fig. 3. Contour maps for affinity at adrenergic α_{1a} , α_{1b} , α_{1d} and α_1 receptors. Positive coefficients (red, 0.003 level) and negative coefficients (blue, -0.003 level) for interaction with the water probe (OH₂) are shown. An unfavourable interaction (positive interaction energy) between a substituent and the probe in regions with negative coefficients is predicted to decrease the affinity (decrease pK_i) and vice versa for positive coefficients. The 5-(1-methylpyrazol-3-yl)-substituted compound **3** is drawn to illustrate the size of the regions.

of the areas varies slightly between the subtypes. Relative to the five-membered heterocycles, the areas for the α_{1a} and α_{1d} subtypes are located in close proximity to the “ortho” position.¹ In contrast, the area in the α_{1b} model is located more towards the “meta” position. This could imply that the “ortho” nitrogens of the five-membered heterocycles are involved in binding to α_{1a} and α_{1d} receptors whereas nitrogens in the “meta” position are involved in binding to α_{1b} receptor. Indeed, the five-membered heterocycles that have nitrogens in the “meta” position and no free lonepair in the “ortho” position like compounds **5**, **14** and **15** have higher affinity for the α_{1b} receptor compared to α_{1a} and α_{1d} . This analysis may also explain the high affinity for α_{1b} receptors observed for the 2-methyl- and 2-ethyl-1,2,3-triazol-4-yl-substituted compounds **6** and **9**. Compound **6** is under-predicted by $0.26 \log_{10}$ units in the model. A 180° rotation around the bond connecting the 1,2,3-triazole moiety with the indole in these compounds

results in substituents with lonepairs of the “meta” nitrogen pointing towards the area of negative coefficients marked with a black arrow in the α_{1b} model, thereby explaining the subnanomolar affinity for α_{1b} receptors for these compounds. This would mean that the assumption that the compounds included in the model bind to the receptor subtypes in a similar manner may not be entirely true. The present results could indicate a different binding mode of some of the heterocyclic substituents in the molecules in the α_{1b} receptor compared to α_{1a} and α_{1d} .

The contour map obtained from the PLS model representing the α_1 model (rat brain membranes) resembles the contour plot of the α_{1b} subtype for the plot of negative coefficients (shown in blue) obtained by the C3 probe (Fig. 2). Similarly, the areas representing specific electrostatic interactions (marked with a black arrow in Fig. 3) are located at similar positions in the α_1 and α_{1b} models. This could indicate that primarily the α_{1b} adrenoceptor subtype is available for radioligand binding in the α_1 assay (rat brain membranes). We have previously hypothesised that the features responsible for high affinity for α_1 receptors for a subset of the compounds listed in Table 1 is a delicate balance between unfavourable steric interactions and favourable electrostatic interactions [19,20]. This hypothesis is supported

¹ Though the use of the terms “ortho” and “meta” is not strictly valid for five-membered rings, we have used the terms within quotation-marks in order to be able to refer to a position in the ring relative to the point of attachment to the indole. This is done because the numbering of the different five-membered heterocycles varies from one heterocycle to the other and dependent on the substitution pattern.

by the present results. Favourable electrostatic interactions between substituents and the OH2 probe in the areas marked with black arrows in Fig. 3 indicate the presence of a hydrogen bond donor in the three α_1 adrenergic receptor subtypes. The exact position of this donor may vary slightly between the subtypes. Furthermore, the areas of positive coefficients (red areas surrounding the methyl group of template molecule 5) in Fig. 2 indicate the presence of a lipophilic pocket or a flexible area in the receptor where substitution is predicted to lead to increased affinity. On the other hand, steric bulk in the area of the indole 6-position and in the area between the indole 5- and 6-positions (blue areas in Fig. 2) is predicted to lead to decreased affinity. Substitution in this area in particular holds a potential for development of α_{1a} adrenoceptor subtype selective compounds.

In contrast to most of the previously reported 3D-QSAR models mentioned in the introduction, the present models are based on one class of compounds only, thereby eliminating the risk of doubtful superimposition of compounds belonging to different chemical classes. The obtained results give rather detailed information about the molecular features of the ligands that contribute to subtype selectivity in a subregion of the α_{1a} , α_{1b} and α_{1d} adrenoceptors. The link between the present phenylindole-based α_1 adrenoceptor antagonists and other classes of compounds have been discussed in a recent publication [19].

6. Conclusion

The 3D-QSAR models for the adrenergic α_{1a} , α_{1b} and α_{1d} receptor subtypes based on a series of 5- and 6-substituted analogues of the antipsychotic drug, sertindole, have revealed different areas in space around the indole skeleton where substitution may lead to enhanced subtype selectivity. The binding affinity for the three α_1 adrenoceptor subtypes seems to benefit from electrostatic interactions between the substituent in the indole 5-position and the receptors. Minor differences in the position of specific electrostatic interactions were observed separating the α_{1b} receptor from the remaining receptor subtypes. However, synthesis of new conformationally restricted analogues with well-defined hydrogen bond acceptors is needed to investigate this topic further. Results indicate a different binding mode for some of the substituents at adrenergic α_{1b} receptors compared to α_{1a} and α_{1d} .

The α_{1a} receptor seems to be more tolerant to large substituents in the area corresponding to the indole 6-position and in the area between the indole 5- and 6-positions. This information may be exploited in the design of new α_{1a} selective compounds.

The contour maps for the α_1 receptors (rat brain homogenate assay) resemble the contour plots for the α_{1b} receptor subtype. This information may be useful when interpreting data from such assays.

References

- [1] J.P. Hieble, D.B. Bylund, D.E. Clarke, D.C. Eikenburg, S.Z. Langer, R.J. Lefkowitz, K.P. Minneman, R.R. Ruffolo Jr., International Union of Pharmacology X. Recommendation for nomenclature of α_1 adrenoceptors: consensus update, *Pharmacol. Rev.* 47 (1995) 267–270.
- [2] H. Zhong, K.P. Minneman, α_1 Adrenoceptor subtypes, *Eur. J. Pharmacol.* 375 (1999) 261–276.
- [3] S.S. O'Malley, T.B. Chen, B.E. Francis, R.E. Gibson, H.D. Burns, J. DiSalvo, M.L. Bayne, J.M. Wetzel, D. Nagarathnam, M. Marzabadi, C. Gluchowski, R.S.L. Chang, Characterization of specific binding of (125 I)L-762,459, a selective α_1 adrenoceptor radioligand to rat and human tissues, *Eur. J. Pharmacol.* 348 (1998) 287–295.
- [4] F. De Paermentier, J.M. Mauger, S. Lowther, M.R. Crompton, C.L. Katona, R.W. Horton, Brain α adrenoceptors in depressed suicides, *Brain Res.* 757 (1997) 60–68.
- [5] A.A. Hancock, α_1 Adrenoceptor subtypes: a synopsis of their pharmacology and molecular biology, *Drug Dev. Res.* 39 (1996) 54–107.
- [6] R.R. Ruffolo Jr., W. Bondinell, J.P. Hieble, α and β adrenoceptors: from the gene to the clinic. 2. Structure–activity relationships and therapeutic applications, *J. Med. Chem.* 38 (1995) 3681–3716.
- [7] J.P. Hieble, W.E. Bondinell, R.R. Ruffolo Jr., α and β adrenoceptors: from the gene to the clinic. 1. Molecular biology and adrenoceptor subclassification, *J. Med. Chem.* 38 (1995) 3415–3444.
- [8] B. Lagu, Identification of α_{1a} adrenoceptor selective antagonists for the treatment of benign prostatic hyperplasia, *Drugs Future* 26 (2001) 757–765.
- [9] B. Kenny, S. Ballard, J. Blagg, D. Fox, Pharmacological options in the treatment of benign prostatic hyperplasia, *J. Med. Chem.* 40 (1997) 1293–1315.
- [10] R.J. Baldessarini, D. Huston-Lyons, A. Campbell, E. Marsh, B.M. Cohen, Do central antiadrenergic actions contribute to the atypical properties of clozapine? *Br. J. Psychiatry Suppl.* 17 (1992) 12–16.
- [11] J.F.J. Lipinski, B.M. Cohen, G.S. Zubenko, C.M. Waternaux, Adrenoceptors and the pharmacology of affective illness: a unifying theory, *Life Sci.* 40 (1987) 1947–1963.
- [12] W.C. Holz, J.P. Hieble, C.A. Gill, R.M. Demarinis, R.G. Pendleton, α Adrenergic agents. 3. Behavioral effects of 2-aminotetralins, *Psychopharmacology* 77 (1982) 259–267.
- [13] J. Arnt, T. Skarsfeldt, Do novel antipsychotics have similar pharmacological characteristics? A review of the evidence, *Neuropsychopharmacology* 18 (1998) 63–101.
- [14] E.P. Prinssen, B.A. Ellenbroek, A.R. Cools, Combined antagonism of adrenoceptors and dopamine and 5-HT receptors underlies the atypical profile of clozapine, *Eur. J. Pharmacol.* 262 (1994) 167–170.
- [15] T.S. Rao, P.C. Contreras, J.A. Cler, M.R. Emmett, S.J. Mick, S. Iyengar, P.L. Wood, Clozapine attenuates *N*-methyl-D-aspartate receptor complex-mediated responses in vivo: tentative evidence for a functional modulation by a noradrenergic mechanism, *Neuropharmacology* 30 (1991) 557–565.
- [16] R.F. Lane, C.D. Blaha, J.M. Rivet, Selective inhibition of mesolimbic dopamine release following chronic administration of clozapine: involvement of α_1 noradrenergic receptors demonstrated by in vivo voltammetry, *Brain Res.* 460 (1988) 398–401.
- [17] M.L. Wadenberg, P. Hertel, R. Fernholm, B.K. Hygge, S. Ahlenius, T.H. Svensson, Enhancement of antipsychotic-like effects by combined treatment with the α_1 adrenoceptor antagonist prazosin and the dopamine D2 receptor antagonist raclopride in rats, *J. Neural Transm.* 107 (2000) 1229–1238.
- [18] M. Ipsen, Y. Zhang, N. Dragsted, C. Han, M.J. Mulvany, The antipsychotic drug sertindole is a specific inhibitor of α_{1a} adrenoceptors in rat mesenteric small arteries, *Eur. J. Pharmacol.* 336 (1997) 29–35.
- [19] T. Balle, J. Perregaard, T. Ramirez, A.K. Larsen, K.K. Sjøby, T. Liljefors, K. Andersen, Synthesis and structure–affinity relationship

- investigations of 5-heteroaryl-substituted analogues of the antipsychotic sertindole. A new class of highly selective α_1 adrenoceptor antagonists, *J. Med. Chem.* 46 (2003) 265–283.
- [20] T. Balle, J. Perregaard, A.K. Larsen, T. Ramirez, K.K. Sjøby, T. Liljefors, K. Andersen, Synthesis and structure–affinity relationship investigations of 5-aminomethyl and 5-carboxamide analogues of the antipsychotic sertindole. A new class of selective α_1 adrenoceptor antagonists, *Bioorg. Med. Chem.*, DOI: 10.1016/S0968-0896(02)-00459-5.
- [21] P.J. Goodford, A computational procedure for determining energetically favorable binding sites on biologically important macromolecules, *J. Med. Chem.* 28 (1985) 849–857.
- [22] GRID, Molecular Discovery Ltd., Oxford, UK, 1998.
- [23] M. Baroni, G. Constantino, G. Cruciani, D. Riganelli, R. Valigi, S. Clementi, Generating optimal linear PLS estimations (GOLPE): an advanced chemometric tool for handling 3D-QSAR problems, *Quant. Struct. Act. Relat.* 12 (1993) 9–20.
- [24] GOLPE 4.5, Multivariate Infometric Analyses, Viale del Castagni 16, Perugia, Italy, 1999.
- [25] G. Cruciani, K.A. Watson, Comparative molecular field analysis using GRID force-field and GOLPE variable selection methods in a study of inhibitors of glycogen phosphorylase b, *J. Med. Chem.* 37 (1994) 2589–2601.
- [26] P.G. De Benedetti, M. Cocchi, M.C. Menziani, F. Fanelli, Theoretical quantitative structure–activity analysis and pharmacophore modelling of selective non-congeneric α_{1a} adrenergic antagonists, *J. Mol. Struct. (Theochem.)* 280 (1993) 283–290.
- [27] P.G. De Benedetti, F. Fanelli, M.C. Menziani, M. Cocchi, R. Testa, A. Leonardi, α_1 Adrenoceptor subtype selectivity: molecular modelling and theoretical quantitative structure–affinity relationships, *Bioorg. Med. Chem.* 5 (1997) 809–816.
- [28] M.C. Menziani, M. Montorsi, P.G. De Benedetti, M. Karelson, Relevance of theoretical molecular descriptors in quantitative structure–activity relationship analysis of α_1 adrenergic receptor antagonists, *Bioorg. Med. Chem.* 7 (1999) 2437–2451.
- [29] D. Barlocco, G. Cignarella, V.D. Piaz, M.P. Giovannoni, P.G. De Benedetti, F. Fanelli, F. Montesano, E. Poggesi, A. Leonardi, Phenylpiperazinylalkylamino-substituted pyridazinones as potent α_1 adrenoceptor antagonists, *J. Med. Chem.* 44 (2001) 2403–2410.
- [30] S. Chen, M. Zu, F. Lin, D. Lee, P. Riek, R.M. Graham, Phe310 in transmembrane VI of the α_{1b} adrenergic receptor is a key switch residue involved in activation and catecholamine ring aromatic bonding, *J. Biol. Chem.* 274 (1999) 16320–16330.
- [31] D.J. Waugh, R.J. Gaivin, M.J. Zuscik, P. Gonzalez-Cabrera, S.A. Ross, J. Yun, D.M. Perez, Phe308 and Phe312 in transmembrane domain VII are major sites of α_1 adrenergic receptor antagonist binding. Imidazoline agonists bind like antagonists, *J. Biol. Chem.* 276 (2001) 25366–25371.
- [32] D.J. Waugh, M.M. Zhao, M.J. Zuscik, D.M. Perez, Novel aromatic residues in transmembrane domains IV and V involved in agonist binding at α_{1a} adrenergic receptors, *J. Biol. Chem.* 275 (2000) 11698–11705.
- [33] M.T. Piascik, D.M. Perez, α_1 Adrenergic receptors: new insights and directions, *J. Pharmacol. Exp. Ther.* 298 (2001) 403–410.
- [34] M. Lapinsh, P. Prusis, A. Gutcaits, T. Lundstedt, J.E. Wikberg, Development of proteo-chemometrics: a novel technology for the analysis of drug–receptor interactions, *Biochim. Biophys. Acta* 1525 (2001) 180–190.
- [35] J. Perregaard, J. Arnt, K.P. Bøgesø, J. Hyttel, C. Sanchez, Non-cateptogenic, centrally acting dopamine D2 and serotonin 5-HT₂ antagonists within a series of 3-substituted 1-(4-fluorophenyl)-1*H*-indoles, *J. Med. Chem.* 35 (1992) 1092–1101.
- [36] J. Perregaard, K. Andersen, J. Hyttel, C. Sanchez, Selective, centrally acting serotonin 5-HT₂ antagonists. 1. 2- and 6-substituted 1-phenyl-3-(4-piperidinyl)-1*H*-indoles, *J. Med. Chem.* 35 (1992) 4813–4822.
- [37] J. Perregaard, B. Costall, Treatment of cognitive disorders, Patent no. PCT/DK92/00063 (WO 92/15303) (1992).
- [38] J. Perregaard, H. Pedersen, K. Andersen, K.P. Bøgesø, Novel indole derivatives, Patent no. 91610055.5 (EP 0 465 398 B1) (1994).
- [39] T.A. Halgren, *J. Comput. Chem.* 17 (1996) 490–641 (Five papers).
- [40] F. Mohamadi, N.G. Richards, W.C. Gouida, R. Liskamp, M. Lipton, C. Caufield, G. Chang, T. Hendrickson, W.C. Still, MacroModel—an integrated software system for modeling organic and bioorganic molecules using molecular mechanics, *J. Comput. Chem.* 11 (1990) 440–467.
- [41] M. Pastor, G. Cruciani, S. Clementi, Smart region definition: a new way to improve the predictive ability and interpretability of three-dimensional quantitative structure–activity relationships, *J. Med. Chem.* 40 (1997) 1455–1464.